Oscillatory phase coupling coordinates anatomically dispersed functional cell assemblies

Ryan T. Canolty[a,b], Karunesh Ganguly[a,b,c,d], Steven W. Kennerley[b], Charles F. Cadieu[b,e], Kilian Koepsell[b,e], Jonathan D. Wallis[b,f], and Jose M. Carmena[a,b,g,1]

[a]Electrical Engineering and Computer Sciences, University of California, Berkeley, CA 94720; [b]Helen Wills Neuroscience Institute, University of California, Berkeley, CA 94720; [c]San Francisco Veterans Affairs Medical Center, San Francisco, CA 94121; [d]Department of Neurology, University of California, San Francisco, CA 94143; [e]Redwood Center for Theoretical Neuroscience, University of California, Berkeley, CA 94720; [f]Department of Psychology, University of California, Berkeley, CA 94720; and [g]Program in Cognitive Science, University of California, Berkeley, CA 94720

Edited* by Nancy J. Kopell, Boston University, Boston, MA, and approved August 27, 2010 (received for review June 11, 2010)

Hebb proposed that neuronal cell assemblies are critical for effective perception, cognition, and action. However, evidence for brain mechanisms that coordinate multiple coactive assemblies remains lacking. Neuronal oscillations have been suggested as one possible mechanism for cell assembly coordination. Prior studies have shown that spike timing depends upon local field potential (LFP) phase proximal to the cell body, but few studies have examined the dependence of spiking on distal LFP phases in other brain areas far from the neuron or the influence of LFP–LFP phase coupling between distal areas on spiking. We investigated these interactions by recording LFPs and single-unit activity using multiple microelectrode arrays in several brain areas and then used a unique probabilistic multivariate phase distribution to model the dependence of spike timing on the full pattern of proximal LFP phases, distal LFP phases, and LFP–LFP phase coupling between electrodes. Here we show that spiking activity in single neurons and neuronal ensembles depends on dynamic patterns of oscillatory phase coupling between multiple brain areas, in addition to the effects of proximal LFP phase. Neurons that prefer similar patterns of phase coupling exhibit similar changes in spike rates, whereas neurons with different preferences show divergent responses, providing a basic mechanism to bind different neurons together into coordinated cell assemblies. Surprisingly, phase-coupling–based rate correlations are independent of interneuron distance. Phase-coupling preferences correlate with behavior and neural function and remain stable over multiple days. These findings suggest that neuronal oscillations enable selective and dynamic control of distributed functional cell assemblies.

neuronal oscillations | neuronal ensembles | spike timing | local field potentials | brain rhythms

Significant progress has been made in understanding the dynamics and response properties of single nerve cells (1, 2) and how they interconnect to form cortical microcircuits (3, 4). More than 60 y ago, however, Donald Hebb hypothesized that the fundamental unit of brain operation is not the single neuron but rather the cell assembly—an anatomically dispersed but functionally integrated ensemble of neurons (5). The individual neurons that compose an assembly may reside in widely separated brain areas but act as a single functional unit through coordinated network activity. Dynamic interactions between multiple assemblies may then give rise to the large-scale functional networks found in mammalian brains (6–8). Despite the theoretical appeal of Hebb's idea (9) and growing empirical evidence of assemblies (10–12), it remains unclear how diverse groups of neurons spanning several cortical regions transiently coordinate their activity to form cell assemblies or how multiple coactive assemblies regulate their interactions to form larger functional networks.

Brain rhythms may play a key role in coordinating neuronal ensembles (13–15), with a dynamic hierarchy of neuronal oscillations modulating local computation and long-range communication (16–18). This hypothesis is supported by evidence that spiking activity depends on the local field potential (LFP) in both hippocampus (19–21) and neocortex (22, 23). In particular, single-neuron spike timing depends on frequency-specific oscillatory LFP phase, both proximal to the neuron (24) and at more distal locations (25). That is, considering the LFP filtered at a given frequency as a sinusoidal waveform, individual neurons tend to emit spikes clustered around a preferred phase, such as the peak (phase: 0 rad or 0°) or trough (phase: π rad or 180°) of the waveform (Fig. S1). In addition to this dependence upon absolute LFP phase, spiking also depends on LFP–LFP phase coupling between distal and proximal sites (26). LFP–LFP phase coupling is estimated from the distribution of phase differences between two LFP signals (Fig. S2*E*) and is a measure of the direct dependence between two signals. In other words, given the frequency-specific phase for one LFP signal, how much does one know about the phase of the other? Spike timing thus appears to depend on neuronal oscillations in both proximal and distal sites as well as on the strength of phase coherence between them. This dependence suggests that the spiking of single neurons is influenced by patterned oscillatory activity occurring in multiple interconnected brain areas as well as the neuron's local cortical environment.

Despite the variety of evidence for LFP–neuron interactions, the role of distributed neuronal oscillations in coordinating single-unit and cell assembly activity remains an open question. We therefore investigated the main hypothesis that oscillations enable computation and long-range communication in distributed brain networks, focusing on the relationship between cell assemblies, proximal and distal LFP phases, and LFP–LFP phase coupling. Specifically, our hypotheses were (*i*) that spike timing in single neurons depends on oscillatory phase coupling across multiple brain areas (Fig. 1 *A–D*), (*ii*) that large-scale patterns of phase coupling synchronize anatomically dispersed neuronal ensembles (Fig. 1 *E–G*), and (*iii*) that sensitivity to distinct brain rhythms or coupling patterns permits selective control of multiple coactive assemblies (Fig. 1 *H–J*).

Results

We tested these hypotheses using existing data sets recorded from macaque frontal cortex. Two monkeys engaged in a brain–machine interface (BMI) task (27) had multiple microelectrode arrays chronically implanted bilaterally in primary motor (M1) and dorsal premotor (PMd) cortex. We also examined data from two monkeys performing a working memory task (28) with acute bilateral recordings in multiple prefrontal areas including dorsal and ventral prefrontal cortex (PFdl and PFvl, respectively), orbitofrontal cortex (PFo), and the dorsal bank of the cingulate sulcus (PFcs).

Author contributions: R.T.C., K.G., S.W.K., C.F.C., K.K., J.D.W., and J.M.C. designed research; R.T.C., K.G., S.W.K., C.F.C., K.K., J.D.W., and J.M.C. performed research; C.F.C. and K.K. contributed new reagents/analytic tools; R.T.C., K.G., C.F.C., K.K., and J.M.C. analyzed data; and R.T.C., K.G., C.F.C., K.K., J.D.W., and J.M.C. wrote the paper.

The authors declare no conflict of interest.

*This Direct Submission article had a prearranged editor.

[1]To whom correspondence should be addressed. E-mail: carmena@eecs.berkeley.edu.

This article contains supporting information online at www.pnas.org/lookup/suppl/doi:10.1073/pnas.1008306107/-/DCSupplemental.

Downloaded by guest on May 6, 2021

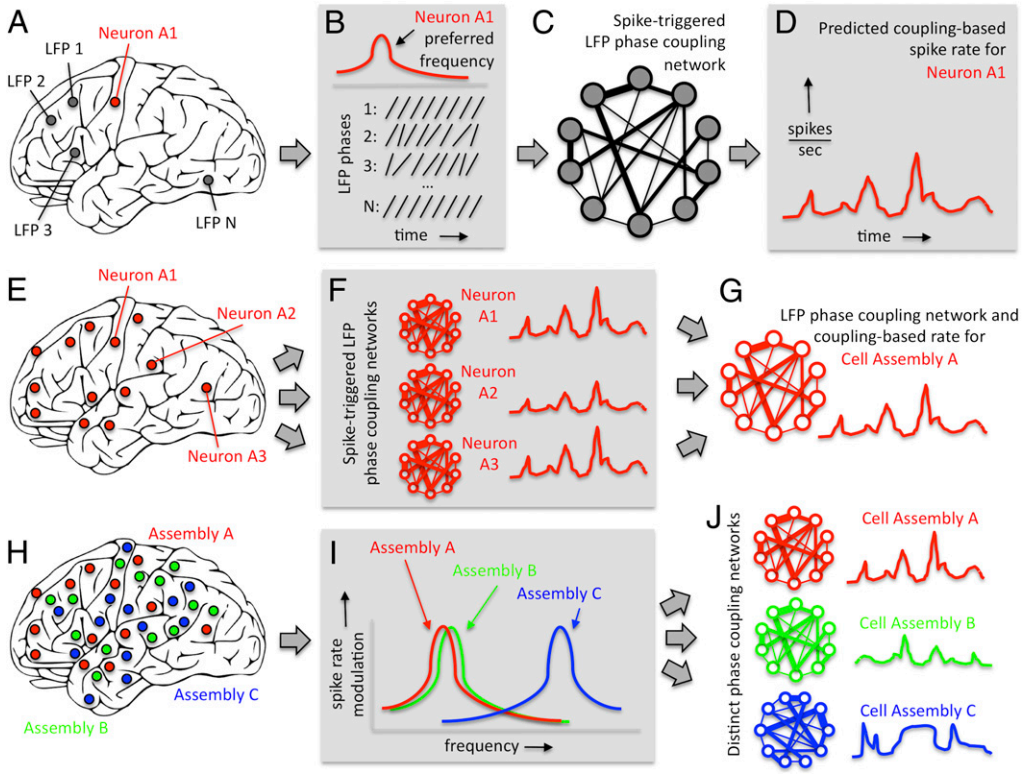

Fig. 1. Patterns of oscillatory phase coupling across multiple brain areas coordinate anatomically dispersed neuronal cell assemblies (schematic). (*A–D*) Hypothesis 1: Spike timing in single neurons depends on frequency-specific oscillatory phase coupling across multiple brain areas. (*A*) Spiking in one area may depend on population activity (local field potentials, LFPs) occurring in multiple areas. (*B*) Many neurons are sensitive to oscillatory LFP activity occurring in particular frequency bands; filtering all LFPs at this frequency and extracting phases can reveal patterns of phase coupling between LFP channels. (*C*) The strength of LFP–LFP phase coupling is different for spike times compared with randomly selected times and defines a neuron's preferred pattern of LFP–LFP phase coupling, similar to a receptive field. That is, when LFP activity matches the neuron's preferred pattern of LFP–LFP phase coupling, the cell spikes more often. (*D*) Given novel LFP phases as input, the model generates a predicted coupling-based spike rate output, which can then be compared with the measured spike rate. (*E–G*) Hypothesis 2: Large-scale patterns of phase coupling synchronize anatomically dispersed neuronal ensembles. (*E*) The procedure described above can be applied to multiple simultaneously recorded neurons. (*F*) Cells that prefer similar LFP–LFP phase-coupling patterns exhibit similar coupling-based rates. (*G*) Shared variability in coupling-based rates is compactly described by a single phase coupling network that defines a cell assembly. That is, it is possible to identify large-scale patterns of LFP–LFP phase coupling (*G*) that explain a significant fraction of the variation in spike rates for a large ensemble of neurons distributed across multiple brain areas. (*H–J*) Hypothesis 3: Differential sensitivity to distinct brain rhythms or coupling patterns permits selective control of multiple coactive assemblies. (*H*) Multiple functional ensembles, each spanning several brain areas, overlap in space. (*I*) Interference between ensembles is minimized when each assembly responds to a different frequency (assemblies A and C) or distinct phase-coupling pattern (assemblies A and B). (*J*) Frequency and pattern selectivity permits dynamic, independent coordination of multiple coactive ensembles.

These data show that neuronal spiking is modulated by widespread LFP activity occurring in distinct frequency bands. In particular, the instantaneous spike rates of most cells are statistically dependent on LFP phases in multiple areas (Fig. S3). Fig. 2*A* shows the dependence of a M1 neuron upon frequency-specific LFP phase in three different brain areas (28 LFP channels in right M1, where the neuron is located; 16 in left M1; and 4 in right PMd). All LFP electrodes were at least 500 μm from the electrode used to record spikes from this neuron, with most electrodes several millimeters away or in the opposite hemisphere. Fig. 2*A* shows the dependence between spike rate and LFP phase as a function of frequency, where the influence of each LFP channel is considered separately. Typical of motor cortical neurons (29), this cell exhibits a strong dependence on the motor high β (25–40 Hz)-band across most electrodes. For example, if we filter the LFP signal recorded from an electrode in left M1 (blue traces in Fig. 2*A*, opposite hemisphere from the neuron), we find that the distribution of all phases over a long time interval is uniform (Fig. S2*B*), but that the distribution of phases that occur at spike times is nonuniform and is clustered around a preferred phase (Fig. S2*C*). This result indicates that spike times and the LFP phase on that channel are statistically dependent and that variation in LFP phase can be converted into a modulation of the expected neuronal spike rate (*SI Methods*). Given the strong modulation in the high β-band for most recorded neurons (29), for the M1–PMd datasets we therefore focused exclusively on the dependence between spikes and 36-Hz phases.

What are the network origins of this dependence? One possibility is that the spiking of this neuron is directly dependent on the LFP activity occurring in the opposite hemisphere, perhaps mediated by direct synaptic contact of projecting transcallosal axons. Alternatively, the neuron may be directly coupled to the proximal LFP through synaptic connections with local interneurons, but not coupled to distal LFP signals, whereas the LFPs from proximal and distal cortical areas are nonetheless in phase coherence. In the second case, spikes and distal LFP phases would not be dependent once proximal LFP phases were known—spikes and distal LFP phases would be conditionally independent given proximal LFP phase. A similar situation may hold for the spike timing dependence on LFP–LFP phase coupling, where such dependence dissolves once conditioned upon proximal phases.

Critically, we cannot answer this question by examining the dependence of spiking upon each LFP channel separately—such an analysis ignores the influence of LFP–LFP interactions and will therefore generate misleading results. Due to widespread network

Downloaded by guest on May 6, 2021

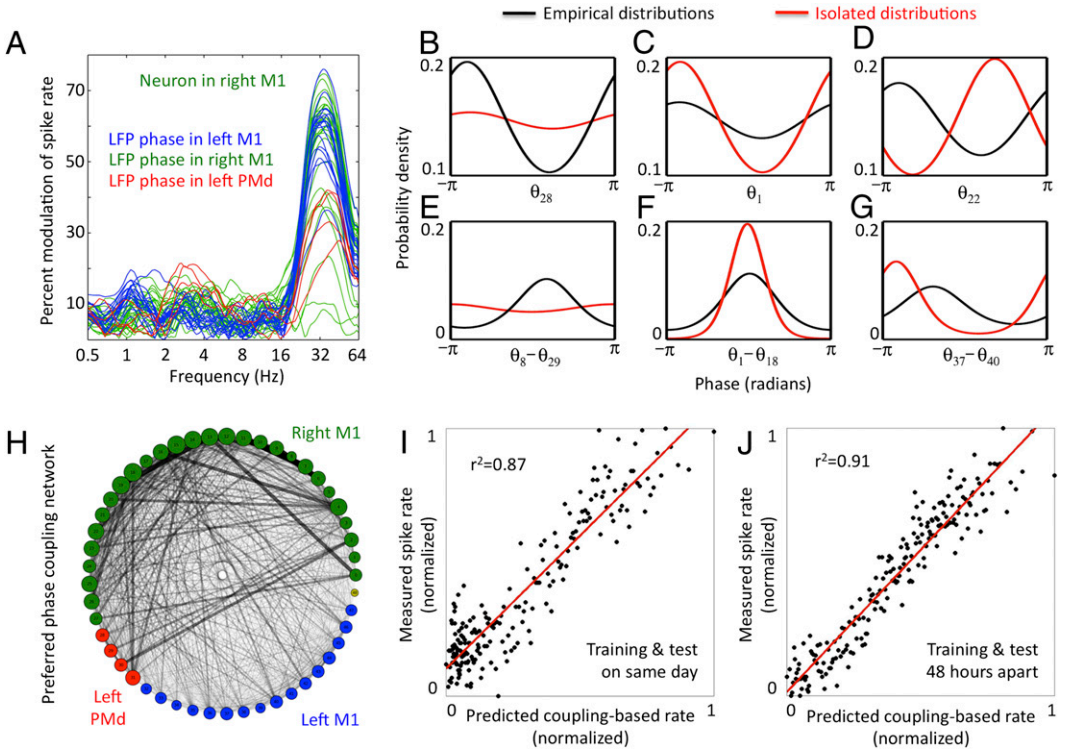

Fig. 2. Spike timing in single neurons depends on oscillatory phase coupling between multiple brain areas. (*A*) Example of a neuron where the probability of spiking depends on frequency-specific LFP phase in multiple areas. The neuron is located in right primary motor cortex (M1). Colored traces represent different LFPs recorded from left M1 (blue), right M1 (green), or left dorsal premotor area (PMd, red). The strong high β (25–40 Hz)-modulation shown here is typical of M1-PMd neurons. (*B–G*) Estimates of spike/LFP interactions depend on the method used and some commonly used techniques may generate misleading results. Examining all LFP signals at once results in differing estimates of phase coupling strength compared with examining pairs of LFP signals separately, as shown by differences between empirical (black) and isolated (red) probability density functions (main text and *SI Methods*; also Figs. S4 and S5). (*H*) Preferred phase coupling network representing 48 LFPs from three brain areas for the M1 neuron shown in *A*. Nodes represent LFP phase variables; links represent the strength of LFP–LFP phase coupling, from weak (light lines) to strong (dark lines). Node size is proportional to the sum of link connection weights entering the node. Strong cross-area coupling remains after conditioning on proximal/distal phases and within-area phase coupling. This preferred pattern of phase coupling acts like an internal, LFP-based receptive field; when the instantaneous pattern of phase coupling between electrodes is close to the preferred coupling pattern, the cell spikes more often. (*I*) The coupling-based spike rate (generated from the preferred LFP–LFP phase coupling pattern learned from training data and instantaneous LFP phases from test data) predicts the measured spike rate (calculated using spike times from test data). (*J*) The relationship between predicted and measured spike rates is stable over multiple days.

connectivity, the phase distribution of one channel, or the distribution of phase differences between two channels, is shaped by the full network of LFP–LFP phase coupling between all channels. We therefore estimated the joint probability distribution over phases using a recently developed multivariate model for circular variables (30) that accounts for these complex network effects (*SI Methods* and Figs. S4 and S5).

Whereas empirical univariate phase distributions are often used to estimate phase concentration and phase coupling, additional influences due to network connectivity bias these estimates. That is, empirical (marginal) probability density functions (PDFs) (black in Fig. 2 *B–G*) differ from the isolated distributions that would be observed if network effects were removed (red in Fig. 2 *B–G*); we term these "isolated distributions," because they single out effects due to coupling between only the phases of interest (*SI Methods*). Isolated distributions provide a more accurate estimate of the direct coupling between two nodes within a larger network than does considering those two nodes alone. For example, Fig. 2*B* shows a case where accounting for network influence reduces our estimate of spike/phase dependence, producing a flatter distribution. In contrast, for some channels removing network effects reveals stronger spike/phase dependence (Fig. 2*C*) or shifts in the preferred phase (Fig. 2*D*). Fig. 2 *E–G* shows similar effects for the phase difference between channels used to estimate the strength of LFP–LFP phase coupling (see also Figs. S4 and S5 for simulations demonstrating these effects).

Surprisingly, the spiking of a single neuron depends on both distal LFP phases and LFP–LFP phase coupling in addition to the proximal LFP phase recorded near the neuronal cell body (Fig. 2*H* and Fig. S3). This dependence indicates that single-unit spiking is related to large-scale network activity patterns rather than simply reflecting local presynaptic phenomena. Importantly, the pattern of phase coupling estimated using all data (baseline coupling) differs from the pattern of phase coupling inferred using spike times alone (spike-triggered coupling). The ratio of these distributions for a given neuron defines its preferred pattern of phase coupling (Fig. 2*H*) and serves as an "internal" receptive field associated with ongoing brain activity, complementing the traditional, stimulus-related "external" receptive field. Each node in Fig. 2*H* represents one LFP electrode, with links between nodes representing LFP–LFP phase coupling. Line shading indicates the strength of LFP–LFP phase coupling. Note that the preferred pattern for this cell exhibits strong coupling between areas (e.g., right M1 and left PMd, shown as links between green and red nodes) as well as strong intra-area coupling (within right M1, green/green links). Importantly, some LFP pairs exhibited increased phase coupling strength, compared with baseline conditions, whereas other LFP pairs displayed decreased coupling (equivalently, increased coupling at a different phase offset).

Downloaded by guest on May 6, 2021

Given a vector of instantaneous phases observed across electrodes at one moment in time, this preferred coupling pattern can be used to generate a phase-coupling–based spike rate prediction. That is, once the joint distribution between spike times and the filtered LFP signals has been learned, a predicted spike rate can be generated from novel LFP input. We call this spike rate prediction, generated from LFP phases alone without reference to the actual spike times, the coupling-based spike rate. Fig. 2 *I–J* shows how this coupling-based rate compares to the actual spike rate when given novel LFP test data (compare with Fig. S6*A* for a neuron from a different subject). Overall, 71.2% of neurons (107/138 for subject P; 51/84 for subject R) exhibited coupling-based rates significantly correlated to measured rates ($P < 0.05$, corrected for multiple comparisons).

Most neurons exhibited preferred phase coupling patterns involving many electrodes in widely separated cortical areas, without the strong localization one might expect from a modular brain architecture. The broad spatial extent of neuron-specific preferred coupling patterns suggests that neurons in different areas may prefer the same pattern and thus have correlated coupling-based rates (Fig. 3 *A* and *B*). In contrast, two neurons with different preferred patterns may exhibit uncorrelated coupling-based rates, even if they are in close proximity (Fig. 3 *C* and *D*). In fact, within a cortical area the correlation between coupling-based rates is independent of interneuron distance (Fig. 3*E*, not significant). In contrast to distance, similarity of neural function predicts coupling-based rate correlations. That is, we can examine the dependence of neuronal spiking on external factors such as target direction in a center-out BMI task (28) to determine neural function, independent of any internal spike/LFP relationships that may exist. Nevertheless, despite assessing these external and internal dependencies separately, on average two neurons with similar directional tuning exhibit stronger coupling-based rate correlations, with correlation magnitude dropping as preferred directions diverge (Fig. 3*F*, $P < 0.01$). Importantly, observing two neurons with correlated spike rates alone is not enough to produce this result; neuronal spiking must also be dependent on the same pattern of LFP–LFP phase coupling (*SI Methods*).

Given that large-scale patterns of phase coupling influence the activity of multiple neurons in similar ways, could changes in these coupling patterns be used to modulate the activity of a coordinated cell assembly? And, if so, could multiple, coactive assemblies be modulated independently? Independent components analysis (ICA) of coupling-based rates reveals a small set of signals responsible for most of the predictive efficacy (Fig. 3*G*, red). That is, the coupling-based rate for each neuron—a spike rate prediction generated from the ongoing LFP signals combined with the pattern of phase coupling preferred by that neuron—can be decomposed as a weighted sum of independent (and thus uncorrelated) signals encoding spike rate variations over time. Each ICA component is associated with a distinct LFP phase coupling pattern and contributes to the weighted sums for many different neurons. Importantly, as shown by Fig. 3*G*, a subset of these components explains spike rate changes across a large ensemble of neurons and can be used for ICA-based denoising (*SI Methods*). Supporting the hypothesis that distributed LFP patterns coordinate cell assembly activity, these ICA-denoised coupling-based rates reveal synchronized ensemble activity within subsets of simultaneously recorded neurons. For example, the correlation matrix between denoised coupling-based rates reveals overlapping clusters of neurons with similar activity (Fig. 3*H*; compare with Fig. S6*B*). That is, simultaneously recorded neurons can be sorted such that neurons with similar rank within a list have correlated changes in predicted spike rates. This shared spike rate variation is evidence that large-scale patterns of phase coupling synchronize anatomically dispersed neuronal ensembles.

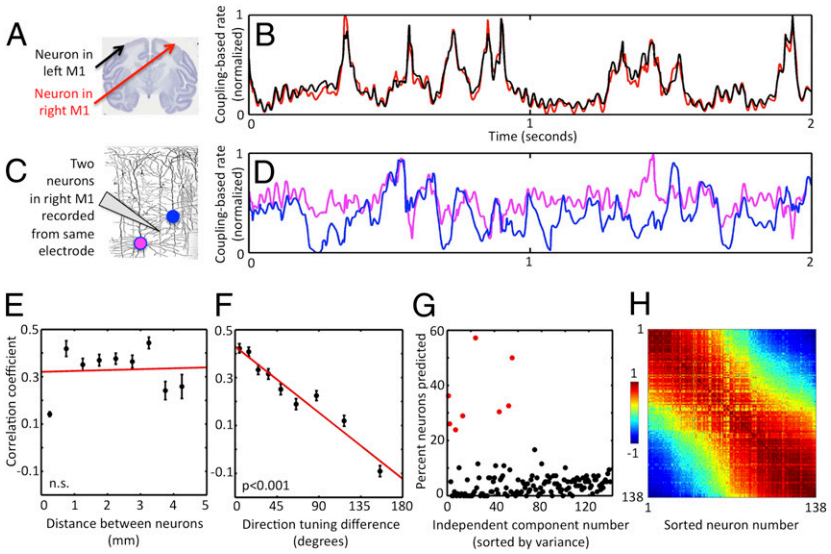

Fig. 3. Large-scale patterns of phase coupling synchronize anatomically dispersed neuronal ensembles. Neurons that prefer similar LFP–LFP phase coupling patterns show correlations between coupling-based spike rates, independent of distance. (*A* and *B*) Two neurons from left and right M1 with correlated coupling-based spike rates. (*C* and *D*) Two neurons recorded from one microelectrode exhibit a weak coupling-based spike rate correlation despite close spatial proximity. (*E*) Within a cortical area, coupling-based spike rate correlations do not depend on interneuron distance (5,716 pairs, n.s.). (*F*) In contrast, motor cortical neurons with similar direction tuning measured during a center-out BMI movement task (28) exhibit coupling-based spike rate correlations (9,413 pairs, $P < 0.001$), suggesting that coupling-based spike rate correlations depend on neural function but not spatial location. (*G*) Shared variability in coupling-based rates is concentrated by independent components analysis (ICA), with a small set of components (red) accounting for most of the predictive value of coupling-based rates (see text). (*H*) Correlation matrix of ICA-denoised coupling-based rates, sorted to identify clusters of neurons with similar activity; e.g., neurons 1–10 form a spatially distributed ensemble with correlated coupling-based rates, have a low correlation with the activity of neurons 61–70, and are anticorrelated with neurons 121–130. The LFP–LFP phase coupling patterns associated with these ICA components explain a portion of the internally generated spike rate variations across an ensemble of anatomically distributed cells and may therefore bind these cells into a functional assembly via Hebbian synaptic modification.

Downloaded by guest on May 6, 2021

Whereas we have shown that spiking depends on large-scale phase coupling patterns, this dependence may be unrelated to perception, cognition, and action. It is therefore of interest that coupling-based rates exhibit event-related changes during behavior. Monkeys engaged in a BMI task (28) must move a cursor to one of eight targets, and significant changes are seen in the trial average of coupling-based rates locked to the onset of a "go" cue (Fig. 4*B*, $P < 0.01$, corrected). Furthermore, as shown by Fig. 4 *C* and *D*, different cue-locked averages (red) correlate with spike-based peristimulus time histograms (PSTHs) (blue) of specific neurons. This correlation is evidence that the relation of spikes to distributed patterns of LFP phase coupling holds during purposeful behavior as well as spontaneous ongoing activity and can be used to predict event-related changes in neural activity.

Finally, for cell assemblies to be effective, multiple ensembles must be able to act in an independent, multiplexed fashion (Fig. 1*H*). One potential mechanism was identified above: Distinct phase-coupling patterns at a given frequency can generate independent modulatory signals that drive different sets of neurons (Fig. 1*I*, cell assemblies A and B, and Fig. 3*H*). Another possibility is that different ensembles tune into distinct brain rhythms, a form of frequency–domain modularity (Fig. 1*I*, assemblies A and C). As in Fig. 2*A*, Fig. 4 *E–H* shows prefrontal neurons with distinct frequency preferences across many areas, whereas Fig. 4*I* shows the sorted optimal frequencies for all 813 frontal neurons examined in this study. Preferred frequencies span a wide range from <0.3 Hz to >40 Hz, such that for any given frequency there exists a large ensemble of neurons modulated by phase coupling patterns occurring at that frequency. Such ensembles experience a common modulatory drive and thus have the potential to operate as a coherent assembly ("fire together, wire together"). Thus, the sensitivity of neurons to (*i*) distinct brain rhythms as well as (*ii*) distinct, single-frequency coupling patterns suggests two mechanisms for the selective control of multiple coactive assemblies.

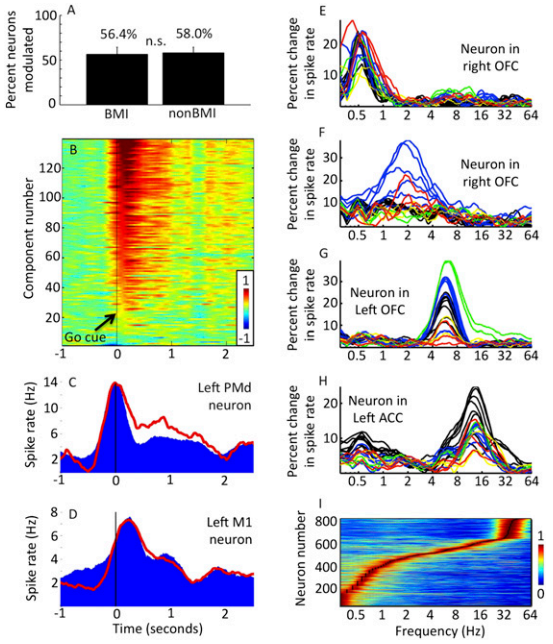

Fig. 4. Phase coupling networks exhibit behavior-related changes and may selectively respond to different frequency bands. (*A*) Monkeys engaged in a brain–machine interface (BMI) task, using some cells (BMI neurons) to drive an on-screen cursor (28). The percentage of neurons exhibiting significant coupling-based rate modulation was the same for BMI and non-BMI groups. (*B*) Predicted spike rates generated by assembly-specific coupling patterns (*SI Methods*) show event-related changes. Time is relative to GO cue onset; the vertical axis shows different independent components sorted by activity level 100 ms after cue onset. (*C*) Peristimulus time histogram (PSTH, blue) for a PMd neuron shows an activity peak at cue onset. The cue-locked average of one coupling-based rate (red) shows event-related changes that correlate with PSTH activity. (*D*) As in *C*, for a M1 neuron and different coupling-based rate. Both PSTH (blue) and coupling-based rate (red) peak ~100 ms after cue. (*E–H*) Different neurons are sensitive to distinct frequencies. Plots show neuronal sensitivity to LFP phase versus frequency (compare with Fig. 2*A*). Colored traces represent LFPs from different areas: right (red) and left (yellow) dorsolateral prefrontal cortex, right (blue) and left (green) orbitofrontal cortex, and left cingulate sulcus (black). (*I*) Eight hundred thirteen neurons from four subjects sorted by preferred frequency (black dots). Horizontal lines show normalized modulation strength from low (blue) to high (red) versus frequency; the broad range of preferred frequencies may enable multiple ensembles to operate with minimal interference.

Discussion

Are oscillations simply epiphenomenal reflections of population activity? Or can fluctuations in electric fields have a causal impact on neuronal networks? Recent studies show that externally generated, experimenter-controlled oscillatory electric fields have a causal impact on hippocampal (31) and neocortical (32) slices in vitro. Importantly, the timing of external stimuli relative to the phase of the oscillating field can affect spike probability and timing (31, 32). Other studies used current injection to simulate synaptic input and show that cellular (33) and network (2) properties interact with the injected current to influence spiking timing (34) and stimulus discriminability (35). Finally, in vivo studies show that depth of processing varies with local oscillatory phase (15, 36, 37) and that oscillatory activity arises from interacting networks of multiple cell subtypes (21, 38–40). Thus, neuronal oscillations clearly have a direct causal impact upon local cortical computation.

In contrast to these local effects, oscillations in distant cortical areas cannot have a direct ephaptic (field-only) influence upon neurons. The dependence of spiking on distal phases and phase coupling shown in this study must therefore rely on synaptic connections mediated by projecting axons. Our findings complement Fries' communication through coherence (CTC) hypothesis (14), where relative phase differences modulate the effective connectivity between two cortical areas (26). Our hypothesis that distributed LFP activity influences spiking activity (Fig. 1 *A–D*) incorporates *N* distinct phase signals simultaneously and can be considered a natural extension of the inherently two-dimensional CTC hypothesis. That is, we show that spiking in single neurons depends on the full pattern of oscillatory phases occurring in multiple brain areas and that phase coupling patterns will therefore have an impact on long-range communication.

The idea that oscillations also play a key role in perception, cognition, and action is strengthened by findings that oscillations are entrained by early sensory (15), motor (41), and linguistic (42) events. This entrainment depends on attention (15, 41) and provides a link to internal processes critical for learning and memory—processes associated with characteristic low-frequency brain rhythms (13, 43). Prior work suggests a relationship between rhythm frequency and the spatial extent of engaged brain networks, with low frequencies binding large-scale networks and high frequencies coordinating smaller networks (44). It is intriguing to speculate on the connection between the fluid, higher-order cognitive processing enabled by prefrontal areas, on the one hand, and the diversity of prefrontal rhythms that may coordinate multiple cell assemblies, on the other. These connections are beyond the scope of this paper, but could be investigated using a similar methodology.

In agreement with prior studies (45, 46), we show above that neurons are sensitive to multiple frequencies. The cellular and network origins of different rhythms are the focus of ongoing research (39), but the period of concatenation hypothesis (47) provides an elegant mechanism that generates the frequency bands observed in neocortex. Each distinct brain rhythm thus generated could exert independent control of different neuronal ensembles. Furthermore,

Downloaded by guest on May 6, 2021

interactions between different frequency bands (16, 17, 48, 49) may provide a mechanism to coordinate the activity of multiple functional assemblies; future research will be required to determine the impact of cross-frequency coupling on spike/LFP interactions.

Here we presented evidence that dynamic patterns of oscillatory coupling across multiple brain areas coordinate anatomically dispersed neuronal cell assemblies. In particular, we found that spike timing depends on distal LFP phases and long-range phase coupling, even after accounting for proximal phase. Different neurons with similar phase-coupling preferences exhibit similar coupling-based rates, independent of interneuron distance. Importantly, this modulation depends on the functional role of neurons and correlates with behavior, suggesting that neuronal oscillations may synchronize anatomically dispersed ensembles actively engaged in functional roles. Finally, we found that frontal neurons are selective for a broad range of frequencies and distinct patterns of phase coupling and thus may provide a mechanism for selective control of multiple coactive assemblies. Together, these findings support the hypothesis that neuronal oscillations play a role in coordinating the functional cell assemblies thought to be responsible for computation and communication in large-scale brain networks.

Methods

A detailed description of the methods is provided in *SI Methods*.

Surgery, Electrophysiology, and Analysis. Two adult monkeys were chronically implanted with multiple microelectrode arrays bilaterally in M1 and PMd and performed a BMI task. Two different monkeys engaged in a working memory task and had acute recordings made from multiple prefrontal areas. The pairwise phase distribution of LFP measurements was modeled using a probabilistic model (30). For each neuron, two models were fitted using either all LFP data or LFP phases occurring at spike times alone and then related using Bayes' rule.

ACKNOWLEDGMENTS. This work was funded by National Institutes of Health Grants R01DA-19028 and P01NS-040813 (to J.D.W.), National Institutes of Health Grant F32MH-081521 (to S.W.K.), National Science Foundation Grants IIS-0941343 (to J.M.C.), IIS-0917342 (to K.K.) and IIS-1010239 (to C.F.C. and K.K.), the US Department of Veterans Affairs and American Heart Association (to K.G.), the Defense Advanced Research Projects Agency Contract N66001-10-C-2008, and the Multiscale Systems Center (to J.M.C.).

1. Kandel E (2000) *Principles of Neural Science* (McGraw–Hill, New York), 4th Ed.
2. Destexhe A, Rudolph M, Paré D (2003) The high-conductance state of neocortical neurons in vivo. *Nat Rev Neurosci* 4:739–751.
3. Shepherd GM, Stepanyants A, Bureau I, Chklovskii D, Svoboda K (2005) Geometric and functional organization of cortical circuits. *Nat Neurosci* 8:782–790.
4. Douglas RJ, Martin KAC (2004) Neuronal circuits of the neocortex. *Annu Rev Neurosci* 27:419–451.
5. Hebb DO (1949) *The Organization of Behavior* (Wiley, New York).
6. Varela F, Lachaux JP, Rodriguez E, Martinerie J (2001) The brainweb: Phase synchronization and large-scale integration. *Nat Rev Neurosci* 2:229–239.
7. Greicius MD, Krasnow B, Reiss AL, Menon V (2003) Functional connectivity in the resting brain: A network analysis of the default mode hypothesis. *Proc Natl Acad Sci USA* 100:253–258.
8. Mesulam MM (1990) Large-scale neurocognitive networks and distributed processing for attention, language, and memory. *Ann Neurol* 28:597–613.
9. Harris KD (2005) Neural signatures of cell assembly organization. *Nat Rev Neurosci* 6: 399–407.
10. Harris KD, Csicsvari J, Hirase H, Dragoi G, Buzsáki G (2003) Organization of cell assemblies in the hippocampus. *Nature* 424:552–556.
11. Riehle A, Grün S, Diesmann M, Aertsen A (1997) Spike synchronization and rate modulation differentially involved in motor cortical function. *Science* 278:1950–1953.
12. Hoffman KL, McNaughton BL (2002) Coordinated reactivation of distributed memory traces in primate neocortex. *Science* 297:2070–2073.
13. Miller R (1991) *Cortico-Hippocampal Interplay and the Representation of Contexts in the Brain* (Springer, New York).
14. Fries P (2005) A mechanism for cognitive dynamics: Neuronal communication through neuronal coherence. *Trends Cogn Sci* 9:474–480.
15. Lakatos P, Karmos G, Mehta AD, Ulbert I, Schroeder CE (2008) Entrainment of neuronal oscillations as a mechanism of attentional selection. *Science* 320:110–113.
16. Lakatos P, et al. (2005) An oscillatory hierarchy controlling neuronal excitability and stimulus processing in the auditory cortex. *J Neurophysiol* 94:1904–1911.
17. Canolty RT, et al. (2006) High gamma power is phase-locked to theta oscillations in human neocortex. *Science* 313:1626–1628.
18. Canolty RT, et al. (2007) Spatiotemporal dynamics of word processing in the human brain. *Front Neurosci* 1:185–196.
19. Bragin A, et al. (1995) Gamma (40-100 Hz) oscillation in the hippocampus of the behaving rat. *J Neurosci* 15:47–60.
20. Chrobak JJ, Buzsáki G (1998) Gamma oscillations in the entorhinal cortex of the freely behaving rat. *J Neurosci* 18:388–398.
21. Klausberger T, et al. (2004) Spike timing of dendrite-targeting bistratified cells during hippocampal network oscillations in vivo. *Nat Neurosci* 7:41–47.
22. Freeman WJ (1975) *Mass Action in the Nervous System* (Academic, New York).
23. Eeckman FH, Freeman WJ (1990) Correlations between unit firing and EEG in the rat olfactory system. *Brain Res* 528:238–244.
24. Jacobs J, Kahana MJ, Ekstrom AD, Fried I (2007) Brain oscillations control timing of single-neuron activity in humans. *J Neurosci* 27:3839–3844.
25. Siapas AG, Lubenov EV, Wilson MA (2005) Prefrontal phase locking to hippocampal theta oscillations. *Neuron* 46:141–151.
26. Womelsdorf T, et al. (2007) Modulation of neuronal interactions through neuronal synchronization. *Science* 316:1609–1612.
27. Ganguly K, Carmena JM (2009) Emergence of a stable cortical map for neuroprosthetic control. *PLoS Biol* 7:e1000153.
28. Kennerley SW, Wallis JD (2009) Reward-dependent modulation of working memory in lateral prefrontal cortex. *J Neurosci* 29:3259–3270.
29. Rubino D, Robbins KA, Hatsopoulos NG (2006) Propagating waves mediate information transfer in the motor cortex. *Nat Neurosci* 9:1549–1557.
30. Cadieu CF, Koepsell K (2010) Phase coupling estimation from multivariate phase statistics. *Neural Comput*, in press. Available at: http://redwood.berkeley.edu/klab/papers/CadieuKoepsell_PCE_NeuralComp.pdf.
31. Fujisawa S, Matsuki N, Ikegaya Y (2004) Chronometric readout from a memory trace: Gamma-frequency field stimulation recruits timed recurrent activity in the rat CA3 network. *J Physiol* 561:123–131.
32. Fröhlich F, McCormick DA (2010) Endogenous electric fields may guide neocortical network activity. *Neuron* 67:129–143.
33. Hutcheon B, Yarom Y (2000) Resonance, oscillation and the intrinsic frequency preferences of neurons. *Trends Neurosci* 23:216–222.
34. Volgushev M, Chistiakova M, Singer W (1998) Modification of discharge patterns of neocortical neurons by induced oscillations of the membrane potential. *Neuroscience* 83:15–25.
35. Schaefer AT, Angelo K, Spors H, Margrie TW (2006) Neuronal oscillations enhance stimulus discrimination by ensuring action potential precision. *PLoS Biol* 4:e163.
36. Kruglikov SY, Schiff SJ (2003) Interplay of electroencephalogram phase and auditory-evoked neural activity. *J Neurosci* 23:10122–10127.
37. Koepsell K, Wang X, Hirsch JA, Sommer FT (2010) Exploring the function of neural oscillations in early sensory systems. *Front Neurosci* 4:53–61.
38. Mitzdorf U (1985) Current source-density method and application in cat cerebral cortex: Investigation of evoked potentials and EEG phenomena. *Physiol Rev* 65: 37–100.
39. Traub RD, Bibbig A, LeBeau FEN, Buhl EH, Whittington MA (2004) Cellular mechanisms of neuronal population oscillations in the hippocampus in vitro. *Annu Rev Neurosci* 27:247–278.
40. Cardin JA, et al. (2009) Driving fast-spiking cells induces gamma rhythm and controls sensory responses. *Nature* 459:663–667.
41. Saleh M, Reimer J, Penn R, Ojakangas CL, Hatsopoulos NG (2010) Fast and slow oscillations in human primary motor cortex predict oncoming behaviorally relevant cues. *Neuron* 65:461–471.
42. Luo H, Poeppel D (2007) Phase patterns of neuronal responses reliably discriminate speech in human auditory cortex. *Neuron* 54:1001–1010.
43. Rizzuto DS, Madsen JR, Bromfield EB, Schulze-Bonhage A, Kahana MJ (2006) Human neocortical oscillations exhibit theta phase differences between encoding and retrieval. *Neuroimage* 31:1352–1358.
44. von Stein A, Sarnthein J (2000) Different frequencies for different scales of cortical integration: From local gamma to long range alpha/theta synchronization. *Int J Psychophysiol* 38:301–313.
45. Whittington MA, Traub RD (2003) Interneuron diversity series: Inhibitory interneurons and network oscillations in vitro. *Trends Neurosci* 26:676–682.
46. Jacobs J, Kahana MJ, Ekstrom AD, Fried I (2007) Brain oscillations control timing of single-neuron activity in humans. *J Neurosci* 27:3839–3844.
47. Kramer MA, et al. (2008) Rhythm generation through period concatenation in rat somatosensory cortex. *PLoS Comput Biol* 4:e1000169.
48. Tort ABL, et al. (2008) Dynamic cross-frequency couplings of local field potential oscillations in rat striatum and hippocampus during performance of a T-maze task. *Proc Natl Acad Sci USA* 105:20517–20522.
49. Tort ABL, Komorowski RW, Manns JR, Kopell NJ, Eichenbaum H (2009) Theta-gamma coupling increases during the learning of item-context associations. *Proc Natl Acad Sci USA* 106:20942–20947.

NEUROSCIENCE
APPLIED PHYSICAL SCIENCES
Downloaded by guest on May 6, 2021